

## One-step synthesis and enhanced blue emission of carbon-encapsulated single-crystalline ZnSe nanoparticles

B. Y. Geng,<sup>a)</sup> Q. B. Du, X. W. Liu, J. Z. Ma, and X. W. Wei

*College of Chemistry and Materials Science, Anhui Key Laboratory of Functional Molecular Solids, Anhui Normal University, Wuhu 241000, People's Republic of China*

L. D. Zhang

*Institute of Solid State Physics, Chinese Academy of Sciences, Hefei 230031, People's Republic of China*

(Received 30 March 2006; accepted 28 May 2006; published online 20 July 2006)

Carbon-encapsulated ZnSe nanoparticles with diameters about 50 nm were synthesized by noncatalytic one-step thermal evaporation method. The ZnSe cores have a wurtzite crystal structure. The as-synthesized products are uniform and composed of single-crystalline ZnSe nanoparticles enwrapped with polycrystalline graphite layers. The photoluminescence measurement of the carbon-encapsulated nanoparticles shows that the blue emission enhances dramatically compared with the naked ZnSe nanoparticles. This synthetic strategy might exploit a favorable route to synthesize carbon-encapsulated semiconductor nanostructures, which are potentially important for optoelectronic nanodevices. © 2006 American Institute of Physics. [DOI: 10.1063/1.2227964]

Since the first report of the nanocrystalline metal particles encapsulated by graphite layers, the filled nanocapsules have drawn much attention in the past decade.<sup>1,2</sup> Most of the filled nanocapsule or the nanocrystalline encapsulated by graphite layers researches are focused on the metal in bulk form.<sup>3,4</sup> It has been anticipated that these carbon-encapsulated nanoparticles will have potential applications in many fields such as magnetic data storage, magnetic toner in xerography, and contrast agent in magnetic resonance imaging.<sup>5,6</sup>

Selenides, as wide-band-gap II-VI semiconductor materials, have been studied extensively due to their wide applications in the fields of light-emitting devices, solar cells, sensors, and optical recording materials.<sup>7-10</sup> Among those, ZnSe is a direct band gap semiconductor, with room-temperature band gap energy and an emission at 2.8 eV, which suggests that ZnSe is a potentially good material for short-wavelength lasers and other photoelectronic devices. Therefore, ZnSe is of great interest as a model material in such forms as thin films, quantum wells, and bulk crystals.<sup>11-14</sup> In addition, ZnSe is of special interest as it exhibits, via quantum confinement effects, tunable blue-ultraviolet (UV) luminescence. The UV range is practically unobtainable for cadmium-based systems such as CdSe, for which the toxicity of cadmium represents an additional disadvantage.<sup>15</sup> ZnSe is one of the promising materials for fabrication of light-emitting devices, such as blue-green laser diodes, and tunable mid-IR laser sources for remote sensing applications.<sup>16</sup> ZnSe also has potential application in optically controlled switching due to its giant photoresistivity.<sup>17</sup>

Many methods have been used to synthesize ZnSe nanoparticles, such as surfactant-assisted chemistry method,<sup>18,19</sup> sonochemical method,<sup>20</sup> solvothermal route,<sup>21,22</sup> and vapor-phase synthesis.<sup>23</sup> It is known that the nanoparticles tend to interact with each other and easily oxidized. In the case of carbon-encapsulated nanocrystals, the seamless outer carbon layers or the onion structures that tightly surround the nanoparticles in the core may offer excellent protection to the

encapsulated nanomaterials. Therefore, it is significant to prepare carbon-encapsulated semiconductor nanoparticles, which are potentially important for optoelectronic and magnetic nanodevices. Here, we report on the preparation of carbon-encapsulated ZnSe nanoparticles from a one-step noncatalytic thermal evaporation route. The synthetic reaction was carried out in a quartz tube furnace using high purity Ar as carrier gas at 1100 °C; toluene and pure ZnSe powders were used as the starting materials. In photoluminescence (PL) spectra, an enhanced blue emission was observed for the carbon-encapsulated ZnSe nanoparticles and the orange emission was quenched after carbon coating on ZnSe nanoparticles.

The carbon-encapsulated ZnSe nanoparticles were prepared using a noncatalytic one-step thermal evaporation route. In a typical experimental procedure, pure ZnSe powder was loaded in a ceramic boat that was kept in the middle of the ceramic tube. The ceramic boat was covered with a quartz plate to maintain a higher vapor pressure and the ceramic tube was inserted in a horizontal tube furnace. Prior to heating, the system was flushed with high purity Ar (99.99%) for 1 h to eliminate O<sub>2</sub> and pumped down to  $5 \times 10^{-2}$  Torr. Then, under a constant flow of high purity Ar gas [60 SCCM (SCCM denote cubic centimeter per minute at STP)], the furnace was rapidly heated up to 1100 °C (about 4 min). At this temperature, the toluene, which was used as a source of carbon to coat the ZnSe nanoparticles, was injected into quartz tube as reported earlier.<sup>24</sup> The total quantity of toluene injected in each run was 3 ml and the optimized flow rate of the toluene is 0.1 ml/min. The whole system was kept at this temperature for 3 h under a constant flow of argon. After the system was cooled down to room temperature, a large piece of gray-black, wool-like product was found on the inner wall of the quartz tube at downstream end.

The morphology of the wool-like product was studied by transmission electron microscopy (TEM) (JEM 200CX). The x-ray powder diffraction (XRD) pattern was recorded on an MXP18AHF (MaC Science Co. Ltd.) x-ray diffractometer with Cu K $\alpha$  radiation ( $\lambda = 1.54178 \text{ \AA}$ ). Raman spectra were obtained by illuminating the sample with the 514.5 nm line of an Ar<sup>+</sup> laser and 1 mW output power of a laser Raman

<sup>a)</sup> Author to whom correspondence should be addressed; electronic mail: bygeng9559@yahoo.com.cn

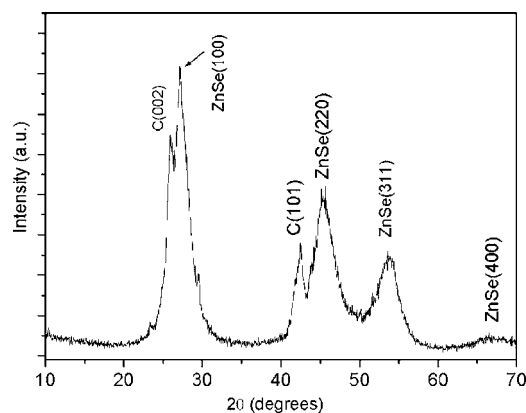


FIG. 1. XRD pattern taken from the synthesized products.

scattering spectrometer (LabRAM HR, Jobin Yvon, France). Spectra of the carbon-encapsulated ZnSe nanoparticles were recorded in the frequency range between 100 and 1800  $\text{cm}^{-1}$ . The structural and elemental analyses of individual carbon-encapsulated ZnSe nanoparticle were performed using high-resolution TEM (HRTEM) (JEOL JEM-2010, 200 kV) and energy-dispersive x-ray fluorescence spectroscopy (EDS) (EDAX, DX-4) attached to the HRTEM. The PL measurements were performed at room temperature using FLS 920 fluorescence spectrophotometer with a Xe lamp.

The typical XRD pattern of the as-synthesized carbon-encapsulated ZnSe nanoparticles is shown in Fig. 1. The analysis of the diffraction pattern indicates that the crystallites exhibit predominantly wurtzite crystal structure. It should be noted that (002) and (101) diffraction peaks from graphite have been found.

Figure 2(a) shows a typical TEM image of as-synthesized products. It can be seen that these nanoparticles are uniform, quasispherical in shape with an average diameter about 50 nm. A higher magnification TEM image inserted in Fig. 2(a) reveals that the as-synthesized products show core-shell structure. The ZnSe nanoparticles are actu-

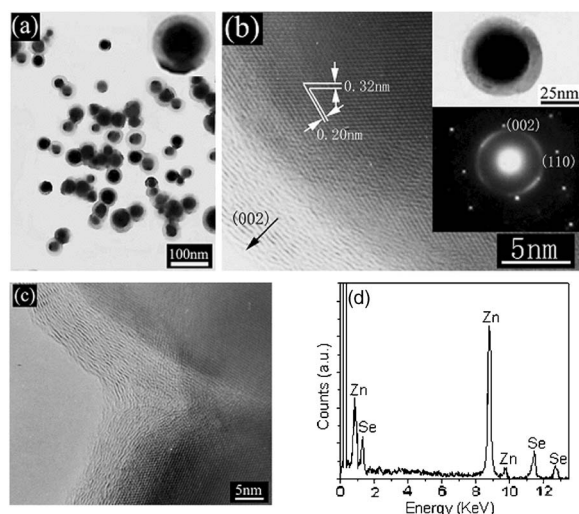


FIG. 2. TEM and HRTEM images of the carbon-encapsulated ZnSe nanoparticles. (a) A typical TEM image of the carbon-encapsulated ZnSe nanoparticles. The inset is a high-magnification TEM image of one carbon-encapsulated ZnSe nanoparticle. (b) HRTEM image of a carbon-encapsulated ZnSe nanoparticle. The insets are overview image [upper in (b)] and SAED pattern [lower in (b)] of this carbon-encapsulated ZnSe nanoparticle. (c) The interface HRTEM image of two combined carbon-encapsulated ZnSe nanoparticles. (d) EDS spectrum of individual carbon-encapsulated ZnSe nanoparticles.

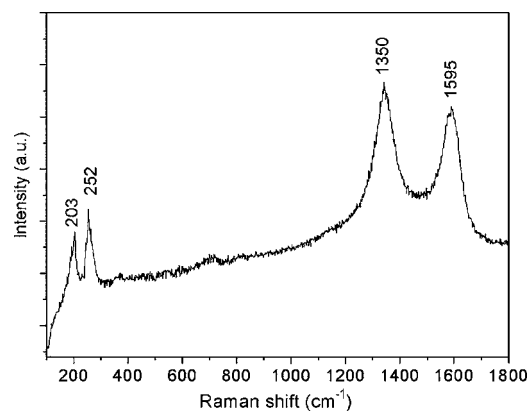


FIG. 3. Raman spectrum of the carbon-encapsulated ZnSe nanoparticles.

ally spherical or nearly spherical in shape with a layer of carbons on the surface.

Figure 2(b) shows representative HRTEM image of a carbon-coated ZnSe nanoparticle with a diameter around 50 nm. An overview image of the carbon-coated ZnSe nanoparticles [upper right inset of Fig. 2(b)] clearly shows a thin carbon layer with thickness about 10 nm on the surface of the ZnSe nanoparticle. The corresponding HRTEM image [Fig. 2(b)] reveals that the ZnSe nanoparticles inside the nanocapsules are structurally uniform and single crystalline. The (100) atomic planes with an interplanar spacing of 0.32 nm and the (220) atomic planes with an interplanar spacing of 0.20 nm are clearly shown. An interface HRTEM image of two combined carbon-encapsulated ZnSe nanoparticles is shown in Fig. 2(c), which further confirms the results as Fig. 2(b).

The selected area electron diffraction (SAED) pattern [lower inset of Fig. 2(b)], taken from the area of the encapsulated nanoparticle, can be indexed as single-crystalline ZnSe along the [100] and [110] zone axes. The diffuse ring capped outside of the ZnSe nanoparticle can be indexed as (002) reflections of graphite. The result of EDS [Fig. 2(d)], which was recorded from different individual encapsulated nanoparticles, indicates that the encapsulated nanoparticle is carbon-encapsulated stoichiometric ZnSe calculated from the quantitative analysis data within experimental error.

Figure 3 shows the Raman spectrum of the carbon-encapsulated ZnSe nanoparticles. Four clear peaks at 203, 252, 1595, and 1350  $\text{cm}^{-1}$  are obtained. The Raman peaks at 203 and 252  $\text{cm}^{-1}$  are attributed to the transverse optic (TO) and longitudinal optic (LO) phonon modes of ZnSe, respectively. From previous reports, the LO phonon frequency of single-crystalline ZnSe film is 254  $\text{cm}^{-1}$  and that of single-crystal ZnSe is 255  $\text{cm}^{-1}$  at room temperature.<sup>25</sup> For ZnSe polycrystalline nanoparticles, the TO and LO phonon frequencies are 210 and 255  $\text{cm}^{-1}$ , respectively, and both give a broad Raman peak due to the high surface-to-volume ratio of small particles. Compared to the results mentioned above, the LO and TO phonon peaks of the carbon-encapsulated ZnSe nanoparticles are both shifted toward lower frequency, which is probably due to the effects of small size and high surface area.

The relatively sharp and symmetric Raman peaks of the ZnSe nanoparticles suggest that the ZnSe nanoparticles are highly crystalline, which is in accord with the HRTEM observations described above. The peak at 1595  $\text{cm}^{-1}$  may be a mixture of  $E_{2g}$  mode which is related to the vibration of

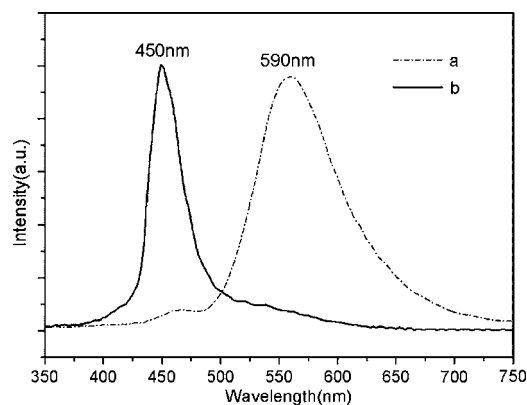


FIG. 4. PL spectra of the naked ZnSe nanoparticles and the carbon-encapsulated ZnSe nanoparticles.

$sp^2$ -bonded carbon atoms in a two-dimensional hexagonal lattice. The peak at  $1350\text{ cm}^{-1}$  is associated with vibrations of carbon atoms with dangling bonds in plane terminations of disordered graphite.<sup>26</sup>

Figure 4 shows the room-temperature PL spectra of the naked ZnSe nanoparticles and the as-synthesized carbon-encapsulated ZnSe nanoparticles. The naked ZnSe nanoparticles display a weak blue emission band at about 450 nm and a strong orange emission band at about 560 nm (Fig. 4, curve a). The weak emission corresponds to a band gap emission of the ZnSe bulk, while the strong emission was assigned to “self-activated” luminescence, probably as a result of some donor-acceptor pairs that are related to Zn vacancy and interstitial states, or associated with dislocations, stacking faults, and nonstoichiometric defects.<sup>27,28</sup> Compared with the PL spectrum of the naked ZnSe nanoparticles, the PL of the carbon-encapsulated ZnSe nanoparticles only has one strong blue emission band at about 450 nm, while the orange emission almost can be neglected, as indicated in Fig. 4, curve b. As the diameters of ZnSe cores are significantly larger than the exciton Bohr diameter, the band gaps of the cores should be similar to that of the bulk ZnSe materials. Therefore, the band around 450 nm is due to the intrinsic emission of ZnSe cores. But it is noted that the intensity of the intrinsic luminescence peak increases remarkably. This change of the PL intensity is attributed to the removal of the electron capture centers on the surface of ZnSe cores and/or the removal of nonradiative decay channels due to the carbon shell.

The importance of the carbon-encapsulated ZnSe nanoparticles is not only the superior structure itself but also the synthesized method of carbon-encapsulated semiconductor nanostructures. The graphite layers can act as chemically inert protecting layers for ZnSe nanoparticles. We also expect to fabricate other morphological carbon-encapsulated nanostructures, such as one-dimensional nanostructures, through controlled experimental conditions. The graphite layers might perform other beneficial effects on nanodevices, such as enhanced stability, for example, of such carbon-encapsulated nanowires against erode and disturb, when used as nanocircuit.

In summary, carbon-encapsulated ZnSe nanoparticles with diameters about 50 nm have been obtained through a noncatalytic thermal evaporation method. The characterizations of structure show that the as-synthesized products are composed of single-crystalline ZnSe nanoparticles capped with polycrystalline graphite layers. PL measurements show

that the blue emission of the as-synthesized carbon-encapsulated ZnSe nanoparticles enhances dramatically. The core/shell structure with polycrystalline carbon shell should be responsible for this PL enhancement. This synthetic strategy might be extended to synthesize other similar nanostructures, which are potentially important for optoelectronic nanodevices.

This work was supported by the Foundation of Key Project of Natural Science of Anhui Education Committee (2006kj041a), Young Teacher Sustentation Project of Anhui (Grant No. 2005jq1041zd), and the Education Department of Anhui Province (2006KJ006TD).

- <sup>1</sup>R. S. Ruoff, D. C. Lorents, B. Chan, R. Malhotra, and S. Subramoney, *Science* **259**, 346 (1993).
- <sup>2</sup>M. Tomita, Y. Saito, and T. Hayashi, *Jpn. J. Appl. Phys., Part 2* **32**, L280 (1993).
- <sup>3</sup>Y. Saito, T. Yoshikawa, M. Okuda, N. Fujimoto, S. Yamamuro, K. Wakoh, K. Sumiyama, K. Suzuki, A. Kasuya, and Y. Nishina, *Chem. Phys. Lett.* **212**, 379 (1993).
- <sup>4</sup>Y. Saito, *Carbon* **33**, 797 (1995).
- <sup>5</sup>S. A. Majetich, J. O. Artman, M. E. Henry, and N. T. Nuhfer, *Phys. Rev. B* **48**, 16845 (1993).
- <sup>6</sup>S. Seraphin, D. Zhou, and J. Jiao, *J. Appl. Phys.* **80**, 2049 (1996).
- <sup>7</sup>M. A. Haase, J. Qiu, J. M. Depuydt, and H. Cheng, *Appl. Phys. Lett.* **59**, 1272 (1991).
- <sup>8</sup>H. Jeon, J. Ding, W. Patterson, and A. V. Nurmikko, *Appl. Phys. Lett.* **59**, 3619 (1991).
- <sup>9</sup>B. Ludolph and M. A. Malik, *Chem. Commun. (Cambridge)* **17**, 1849 (1998).
- <sup>10</sup>Y. W. Jun, J. E. Koo, and J. Cheon, *Chem. Commun. (Cambridge)* **14**, 1243 (2000).
- <sup>11</sup>J. Gutowski, P. Michler, H. I. Ruckmann, H. G. Breunig, M. Rowe, K. Sebal, and T. Voss, *Phys. Status Solidi B* **234**, 70 (2002).
- <sup>12</sup>J. A. Garcia, A. Remon, A. Zubiaga, V. S. Munoz, and C. T. Martinez, *Phys. Status Solidi A* **194**, 338 (2002).
- <sup>13</sup>E. Tournie, C. Morhain, G. Neu, J. P. Faurie, R. Triboulet, and J. O. Nday, *Appl. Phys. Lett.* **68**, 1356 (1996).
- <sup>14</sup>Y. Jing, X. M. Meng, W. C. Yiu, J. Liu, J. X. Ding, C. S. Lee, and S. T. Lee, *J. Phys. Chem. B* **108**, 2784 (2004).
- <sup>15</sup>P. Reiss, G. Quemard, S. Carayon, J. Bleuse, F. Chandezon, and A. Pron, *Mater. Chem. Phys.* **84**, 10 (2004).
- <sup>16</sup>S. B. Mirov, V. V. Fedorov, K. Graham, I. S. Moskalev, V. V. Badikov, and V. Panyutin, *Opt. Lett.* **27**, 909 (2002).
- <sup>17</sup>N. Kouklin, L. Menon, A. Z. Wong, D. W. Thompson, J. A. Woollam, and P. F. Williams, *Appl. Phys. Lett.* **79**, 4423 (2001).
- <sup>18</sup>B. Ludolph, M. A. Malik, P. O'Brien, and N. Revaprasadu, *Chem. Commun. (Cambridge)* **17**, 1849 (1998).
- <sup>19</sup>N. Kumbhojkar, S. Mahamuni, V. Leppert, and S. H. Sisbud, *Nanostruct. Mater.* **10**, 117 (1998).
- <sup>20</sup>J. J. Zhu, Y. Kolytyn, and A. Gedanken, *Chem. Mater.* **12**, 73 (2000).
- <sup>21</sup>J. H. Zhan, X. G. Yang, W. X. Zhang, D. W. Wang, Y. Xie, and Y. T. Qian, *J. Mater. Res.* **15**, 629 (2000).
- <sup>22</sup>Q. Peng, Y. J. Dong, and Y. D. Li, *Angew. Chem., Int. Ed.* **42**, 3027 (2003).
- <sup>23</sup>D. Sarigiannis, J. D. Peck, and T. J. Mountziaris, *Appl. Phys. Lett.* **80**, 4024 (2002).
- <sup>24</sup>H. S. Qian, F. M. Han, B. Z. Zhang, Y. C. Guo, J. Yue, and B. X. Peng, *Carbon* **42**, 761 (2004).
- <sup>25</sup>T. J. Mountziaris, J. D. Peck, S. Stoltz, W. Y. Yu, A. Petrou, and P. G. Mattocks, *Appl. Phys. Lett.* **68**, 2270 (1996); G. Lermann, T. Bischof, A. Materny, W. Kiefer, T. Kummell, G. Bacher, A. Forchel, and G. Landwehr, *J. Appl. Phys.* **81**, 1446 (1997); D. Sarigiannis, J. D. Peck, G. Kioseoglou, A. Petrou, and T. J. J. Mountziaris, *Appl. Phys. Lett.* **80**, 4024 (2002).
- <sup>26</sup>M. W. Shao, Q. Li, J. Wu, B. Xie, S. Y. Zhang, and Y. T. Qian, *Carbon* **40**, 2961 (2002).
- <sup>27</sup>A. Bukaluk, M. Trzcinski, F. Firszt, S. Legowski, and H. Meczynska, *Surf. Sci.* **175**, 507 (2002); J. F. Suyver, S. F. Wuister, J. J. Kelly, and A. Meijerink, *Phys. Chem. Chem. Phys.* **4**, 5445 (2002).
- <sup>28</sup>X. B. Zhang, K. L. Ha, and S. K. Hark, *Appl. Phys. Lett.* **79**, 1127 (2001); X. T. Zhang, Z. Liu, K. M. Ip, Y. P. Leung, Q. Li, and S. K. Hark, *J. Appl. Phys.* **95**, 5752 (2004).